RI 9450

REPORT OF INVESTIGATIONS/1993

Early Detection of Insulation Failure in Electric Motors

By Gerald T. Homce

UNITED STATES DEPARTMENT OF THE INTERIOR

BUREAU OF MINES

Mission: As the Nation's principal conservation agency, the Department of the Interior has responsibility for most of our nationally-owned public lands and natural and cultural resources. This includes fostering wise use of our land and water resources, protecting our fish and wildlife, preserving the environmental and cultural values of our national parks and historical places, and providing for the enjoyment of life through outdoor recreation. The Department assesses our energy and mineral resources and works to assure that their development is in the best interests of all our people. The Department also promotes the goals of the Take Pride in America campaign by encouraging stewardship and citizen responsibility for the public lands and promoting citizen participation in their care. The Department also has a major responsibility for American Indian reservation communities and for people who live in Island Territories under U.S. Administration.

Report of Investigations 9450

Early Detection of Insulation Failure in Electric Motors

By Gerald T. Homce

UNITED STATES DEPARTMENT OF THE INTERIOR

BUREAU OF MINES

Library of Congress Cataloging in Publication Data:

Homce, Gerald T.

Early detection of insulation failure in electric motors / by Gerald T. Homce.

p. cm. — (Report of investigations; 9450)

Includes bibliographical references (p. 16).

Supt. of Docs. no.: I 28:23.9450.

1. Squirrel cage motors—Reliability—Mathematical models. 2. Electric motors—Insulation—Reliability. 3. Mining machinery—Electric driving—Reliability. I. Title. II. Series: Report of investigations (United States. Bureau of Mines); 9450.

TN23.U43 [TK2785] 622 s—dc20 [621.46] 92-5710 CIP

CONTENTS

ILLUSTRATIONS

TABLES

TABLES—Continued

Page

UNIT OF MEASURE ABBREVIATIONS USED IN THIS REPORT

A	ampere	mA	milliampere
°C	degree Celsius	μs	microsecond
deg	degree	pu	per unit
h	hour	V	volt
hp	horsepower	W	watt
kW	kilowatt		

DISCLAIMER

Reference to specific products does not imply endorsement by the U.S. Bureau of Mines.

EARLY DETECTION OF INSULATION FAILURE IN ELECTRIC MOTORS

By Gerald T. Homce[1]

ABSTRACT

A system capable of monitoring mine electrical power systems and detecting impending component failure could significantly improve power system safety and reduce unscheduled equipment downtime. Such monitoring would require a method of evaluating electrical parameters, calculated from terminal values, for indications of component deterioration. The U.S. Bureau of Mines has targeted electrical failure of squirrel cage induction motors and examined the use of mathematical models to aid in this evaluation. The initial stage of this work is complete, and has produced polynomial networks called adaptive learning networks (ALN's) that can detect and quantify winding insulation leakage simulated on laboratory motors. In this modeling process, empirical data from laboratory motors were used to select the electrical parameters most significant for assessing motor conditions, and mathematical expressions relating these parameters to simulated deterioration were formed. ALN's developed thus far can process readily measured motor terminal information and quantify power and current levels of laboratory-simulated leakage to within 1% and 3% of full load values, respectively, for motors in the 10- to 150-hp size range. The next stage of this research is validation of these ALN's for actual motor failures; this stage is currently underway, using accelerated life testing of laboratory motors.

[1]Electrical engineer, Pittsburgh Research Center, U.S. Bureau of Mines, Pittsburgh, PA.

INTRODUCTION

BACKGROUND

Previous U.S. Bureau of Mines research investigated the benefits of using continuous monitoring techniques to evaluate the condition of power system components. Initial studies considered components such as ac and dc motors, power cables, transformers, rectifiers, and capacitor banks, and provided two important findings. Numerous electrical-system-related accidents and significant equipment downtime result from electrical component failure, and time-dependent deterioration of the dielectric properties of insulation accounts for the majority of such failures. Therefore, it was suggested that early detection of deterioration in mine electrical system components could significantly improve system safety and reduce unscheduled equipment downtime. Additional results of this research include the proposal of a methodology for early deterioration detection, development of a computer-based system to detect and analyze the electrical signatures of component deterioration, identification of numerous characteristics for electrical system deterioration, and confirmation of these characteristics by laboratory and field data collection (*1*).[2]

In an independent research program, this work was continued; the relationships between electric motor deterioration mechanisms and their resulting electrical signatures were analyzed, and a classification algorithm for insulation deterioration on motor systems was developed (*2*). Recent Bureau-funded efforts in this area addressed the refinement of the above algorithm, produced several computer models to simulate power system and induction motor operation under deteriorated conditions, and identified deterioration characteristics of induction motor windings (*3*).

The research programs just described produced information that can be used to form a theoretical basis for the detection of low-level insulation deterioration. Additionally, the responses of numerous electrical parameters to various levels and types of cable and motor deterioration were documented. Upon completion of these various programs, however, this information had not yet been successfully implemented in a practical deterioration detection system. Although some generalizations were made regarding specific parameters, and a deterioration classification algorithm was developed for a limited number of cable-connected motor system conditions, a method to detect the state of electrical deterioration was not yet available. This situation prompted the initiation of in-house research at the Bureau to develop such a system for typical mine equipment motors. The work was done in support of two Bureau goals: to provide a safe work environment for miners and to reduce the cost of coal production.

[2]Italic numbers in parentheses refer to items in the list of references preceding the appendix.

ADAPTIVE LEARNING NETWORK[3] APPROACH TO FAILURE DETECTION

Information available from past research suggests that mathematical relationships using measurable parameters can be used to identify electrical insulation deterioration. However, the identification of appropriate input information and derivation of suitable relationships is a complex task. Subject Bureau in-house research utilized an empirical data-modeling approach to this problem, employing commercially available data-modeling software and laboratory-generated power system information to create the necessary relationship(s).

PNETTR-4X[4] (Polynomial NETwork TRainer version 4X), a modeling software package, forms polynomial networks called adaptive learning networks (ALN's) from training data (*4*). Input data are typically multiple sets of measured or calculated quantities that represent a physical process to be modeled. For this research, such data are electrical parameters extracted from laboratory motors undergoing simulated insulation deterioration. PNETTR selected those parameters most significant for modeling motor operation and created ALN's relating the parameters to dependent variables, in this case, insulation deterioration severity. Figure 1 illustrates the use of this methodology to create the basis for an insulation deterioration detection system.

This report describes the results of the first stage of research to develop a practical on-line motor monitoring system for early detection of impending failure. The report includes PNETTR software use, laboratory data collection, development of ALN's for simulated insulation leakage detection, and initiation of a second stage, validation of ALN's using accelerated life testing.

[3]"Adaptive learning network" and "ALN" are registered trademarks of the General Research Corp., McLean, VA.

[4]"PNETTR-4X" is a registered trademark of General Research Corp., McLean, VA.

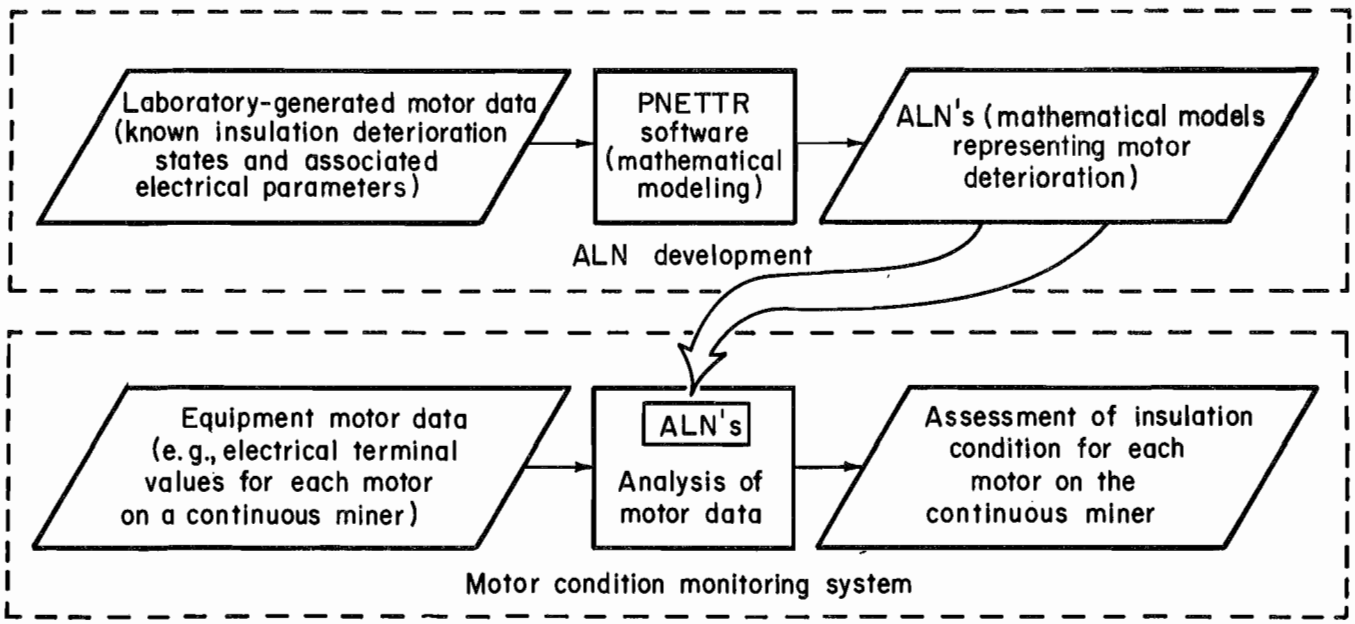

Figure 1.—Methodology for creation of deterioration-detection ALN's.

PNETTR-4X MODELING SOFTWARE

PNETTR-4X is a data-modeling software package marketed by General Research Corp. It can create a polynomial network or ALN to represent a physical process (*4*). PNETTR builds ALN's selecting only those input variables that are necessary for accurate modeling.

The data base required for modeling must include quantities to be used for both dependent and independent variables. ALN's are the mathematical functions that relate some or all of the available independent variables to one or more dependent variables. Although the overall modeling process is unsupervised, the user can significantly alter the final form of an ALN through numerous control options that can restrict modeling flexibility, limit use of data base information, and affect network evaluations that are part of the modeling process. Note that the term "adaptive learning network" indicates only that the polynomial network adapts to the data base during the modeling process. Once formed, a given ALN is fixed.

PNETTR assumes no particular model structure, but creates series-parallel networks of polynomials and generates coefficients solely from a data base. The individual elements of the networks are polynomials, each with up to three different input values. The terms of all polynomials generated by PNETTR are taken from the following general expression:

$$Y = A_0 + A_1X_1 + A_2X_2 + A_3X_3 + A_4X_1X_2 + A_5X_1X_3 + A_6X_2X_3 + A_7X_1^2 + A_8X_2^2 + A_9X_3^2 + A_{10}X_1^3 + A_{11}X_2^3 + A_{12}X_3^3.$$

Usually, only a few of the possible terms will be used in an element, but both the networking of elements and the selection of polynomial terms can range from quite simple to extremely complex. Figure 2 illustrates several possible element connections within an ALN (*4*).

ALN's have been used successfully in numerous fields to model physical processes from observable variables. Several examples are signal processing, pattern recognition, materials testing, geophysical sciences, process control, flight control, health sciences, and economics.

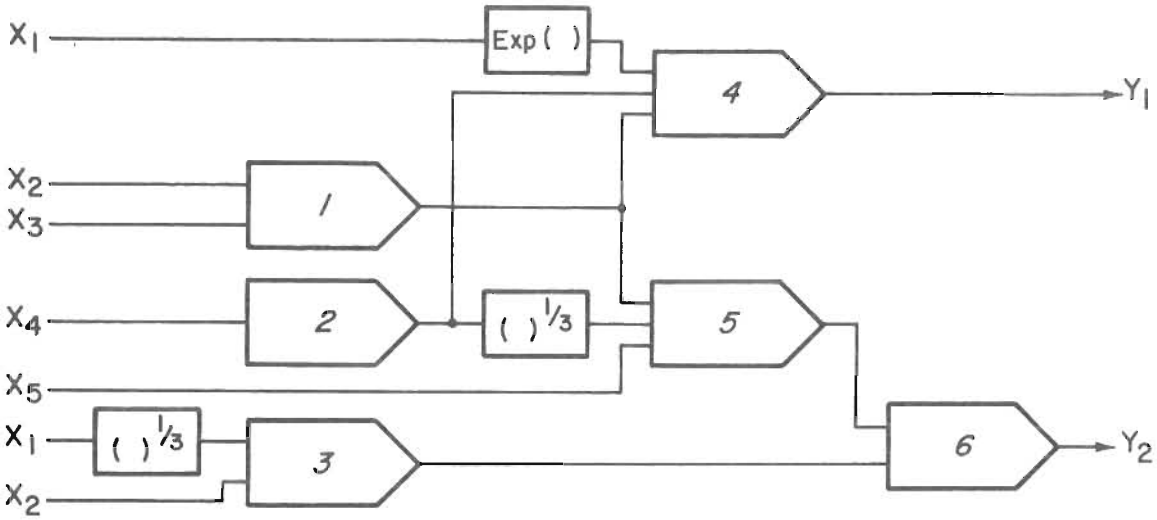

Figure 2.—Possible element connections for ALN. Each element (numbered block) is a polynomial, with up to three input variables. Blocks with parentheses are intermediate operations performed on individual input variables.

DATA COLLECTION

The use of empirical information for modeling motor deterioration necessitates laboratory data collection under well-controlled conditions. Laboratory facilities required for such data collection include an appropriate power system, test motors, instrumentation to monitor the system, and some method to collect and organize the desired information.

Collection of motor data for this research was conducted in the Bureau's Mine Electrical Laboratory. Motor-alternator sets powered by a motor test station and loaded by a bank of resistors were used to generate the required power system terminal information. A bank of resistors was connected to the motor leads through a variable transformer to simulate current leakage (insulation deterioration) across various points on the motor system. Window-type current transformers and isolation potential transformers measured electrical signals from the system terminals and supplied this analog information to a data-acquisition computer.

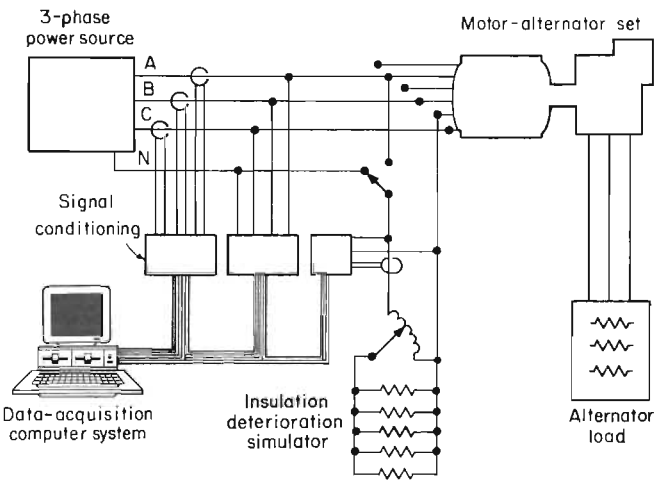

Figure 3.—Layout of Mine Electrical Laboratory power system equipment and data-acquisition hardware used for motor data generation.

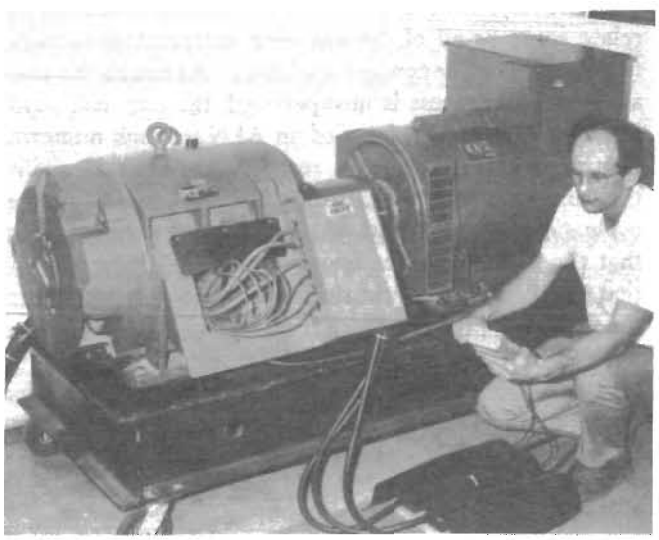

Figure 4.—Motor-alternator set (150 hp, 150 kW) used for motor data generation. (Photo credit: R. Wayne Denlinger, engineering technician, Pittsburgh Research Center.)

The extensive laboratory data collection necessary for empirical modeling requires computer hardware and software that enable researchers to sample instrumentation signals, process the signals to obtain desired electrical values, sort and select specific information, and create data files for input to PNETTR. Early work in this program employed custom written software on a VAX computer cluster to meet these requirements. This system was later supplemented by a desk-top-computer-based system that streamlined the data-collection process and significantly reduced the time necessary to model each motor.

Figure 3 shows the overall layout of the laboratory power system equipment and data-acquisition hardware. Figure 4 shows a motor-alternator set equipped with a 150-hp motor used for data generation.

DEVELOPMENT OF MOTOR FAILURE DETECTION ALN's

GENERAL

Prior to data collection and empirical modeling of electric motor operation, a number of basic decisions must be made regarding the types of motors involved, power system conditions, specific modeling techniques, and the overall approach to monitoring. It is, therefore, necessary to describe the major assumptions and options selected that have focused efforts for this research, as well as the logic behind the selections.

The components targeted are three-phase squirrel cage induction motors, which are the most widely used electric machines in mining operations (*5*). Consequently, deterioration of brushes, slip rings, commutators, and similar components absent in this type of motor was not considered. Additionally, mechanical deterioration such as bearing wear and stator or rotor structural failure was not included in this research.

Electrical failure often originates with the breakdown of insulation and subsequent leakage of current through an abnormal path, eventually resulting in a fault (*1*). Insulation breakdown may be due to any of numerous deterioration mechanisms arising from electrical, thermal, mechanical, or environmental stresses. The development of leakage current paths, however, is the common result of all these processes, and is the effect that directly leads to electrical failure of motors.

The process of insulation breakdown is used to quantify progressive deterioration of induction motors. Deterioration severity is indicated by the level of current flowing and power dissipated in an abnormal path. Such leakage current can seldom be precisely located or directly measured in the field, but it is readily controlled and measured in laboratory simulations. Therefore, laboratory simulations were used in conjunction with PNETTR to establish empirical relationships (ALN's) between deterioration current and power levels and readily measured electrical values.

The laboratory hardware and software described previously were used to generate data for the modeling process. Information such as voltage and current phasors for each phase and deterioration characteristics was sampled during steady-state motor operation, that is, a condition under which terminal information is sufficiently stable to allow reliable ALN analysis (further defined later in this report). All electrical parameters for each sample were derived from the voltage and current phasors, and were candidate input variables to the modeling process, while simulated deterioration levels were dependent variables for the sample.

Data collection and modeling produced ALN's, which are continuous functions relating electrical parameters to deterioration levels. This modeling approach was selected because deterioration current and power levels have a mathematical relationship to specific electrical features. In addition, it does not require selection of a cutoff deterioration level to define a good or bad condition. Further, it provides trend information prior to failure, which will be essential in using motor-condition monitoring systems to accurately anticipate failures.

The ALN's created with PNETTR should ideally determine deterioration presence and level independent of as many variable power system factors as possible, such as leakage level and location, motor load, winding temperature, and bus voltage imbalance. ALN's should also be applicable to systems with motors different from those on which the training data were generated, within reasonable size and design limitations. This ALN "generality" is an important concept for actual application of motor monitoring, in that a specific motor would not require extensive laboratory testing to be successfully monitored in the field. Further, ALN's would be most useful if no "new condition" baseline were needed for a motor to be monitored.

The following sections detail the procedures used for empirical modeling with PNETTR, results of this modeling, and a summary of important ALN characteristics.

EMPIRICAL MOTOR DATA

Independent variables for modeling include measured three-phase voltage and current values as well as the calculated values of system impedance; symmetrical

components for voltage, current, and impedance; system power; and power factor. For each of the complex values used, four separate quantities exist in the data file: rectangular x component, rectangular y component, polar magnitude, and polar angle. This broadens the number of candidate input variables from which PNETTR may choose and reduces the chance of missing subtle parameter variations that may prove valuable for modeling. Simulated leakage current levels were also measured for each sample. Along with calculated deterioration power values, they became the dependent variables in PNETTR data files. Additional information recorded for each sample includes motor stator temperature and the magnitude of power output by the alternator, which directly represents motor load level. Each sample taken represents one of many different conditions simulated for each motor, and includes all of the above described information. Tables 1 and 2 show an example of all information for one sample of motor data, as used in PNETTR modeling.

Table 1.—Example of test condition information[1]

Parameter	*Value*
Observation identification	Time and date or sequential numbering.
Voltage at leakage path, pu	1.732.
Current at leakage path, pu	0.100.
Power at leakage path, pu	0.173.
Motor load, pu	0.8539.
Deterioration path grounding status	No ground connection.
Deterioration path grounding code	1.
Deterioration path identification	A-B.
Deterioration path code	1.

[1]This list and the one in table 2 will serve as one of many observations that make up input data for PNETTR modeling.

FAILURE DETECTION ALN's

Initial motor modeling under this program focused on the effects of individual specific system conditions on ALN accuracy. Typically, only one parameter, such as deterioration type, location, and severity or motor loading, was varied for each investigation. In subsequent testing, a wide range of motor system conditions were used as input to the modeling process, including the use of a single model to evaluate several different motors. This preliminary work established the feasibility of modeling simulated insulation leakage on three-phase squirrel cage induction motors using PNETTR, and formed the basis for further development and refinement of ALN's targeting motors ranging from 10 to 150 hp.

Table 2.—Electrical parameters[1]

Parameters[2]	Polar magnitude, pu	Polar angle, deg	Rectangular x, pu	Rectangular y, pu
Voltage A-n	0.998	0.0	0.998	0.000
Voltage B-n	.996	239.9	-.500	-.862
Voltage C-n	.995	120.9	-.511	.854
Current A	1.038	337.7	.960	-.393
Current B	1.077	211.7	-.916	-.566
Current C	.950	91.5	-.025	.949
Impedance A	.962	22.3	.890	.364
Impedance B	.925	28.2	.816	.437
Impedance C	1.047	29.4	.913	.514
Positive sequence voltage	.996	.3	.996	.005
Negative sequence voltage	.006	342.1	.006	-.002
Zero sequence voltage	.005	214.1	-.004	-.003
Positive sequence current	1.020	333.7	.914	-.452
Negative sequence current	.074	57.7	.039	.062
Zero sequence current	.007	332.5	.006	-.003
Positive sequence impedance	.977	26.6	.874	.437
Negative sequence impedance.	.081	284.3	.020	-.079
Zero sequence impedance	.704	241.6	-.335	-.619
Complex power A	1.035	22.3	.958	.392
Complex power B	1.073	28.2	.946	.507
Complex power C	.945	29.4	.823	.464
Average complex power	1.016	26.5	.909	.453

[1]All parameters listed here are derived from one sample of terminal values measured on a 10-hp motor. This list and the one in table 1 will serve as one of many observations that make up input data for PNETTR modeling.

[2]Power factor A = 0.9254, power factor B = 0.8815, power factor C = 0.8713, and average power factor = 0.8928.

Data generated for this research simulate insulation leakage across all possible combinations of seven locations on motor windings. Connection points include phase conductors (motor line terminals), midpoints of each delta-connected winding within the motor, and the power system neutral (G). A variable resistance placed between selected points created leakage currents, as illustrated in figure 5, including simulation of all the following paths:

A-B	B-C	C-A
A-G	B-G	C-G
A-a	B-a	C-a
A-b	B-b	C-b
A-c	B-c	C-c
a-b	b-c	c-a
a-G	b-G	c-G

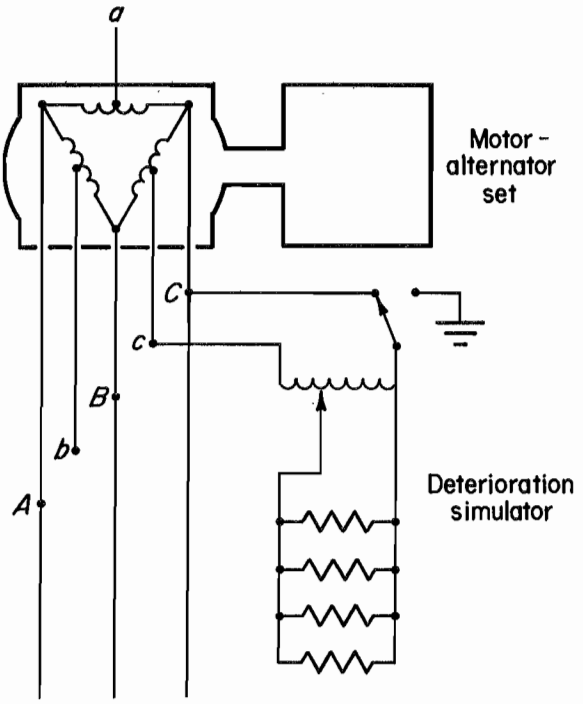

Figure 5.—Deterioration simulation for laboratory data collection.

Simulations included current levels of 0.00 to 0.10 per unit (pu)[5] at 0.01-pu increments, as well as 0.15, 0.20, and 0.25 pu. Such levels represent 122 mA to 3.05 A on a 10-hp 460-V motor, and 1.73 to 43.25 A on a 150-hp 460-V motor.

The lower limit of these leakage simulations was ultimately dictated by practical lower limits of resolution for the modeling techniques and data-collection hardware.

The upper limit was selected based on the lower trip level commonly found on motor circuit protection devices. The actual leakage current and power levels possible in a motor prior to a complete failure are not yet known. Undocumented reports, however, suggest that motors have remained in service with electrical imbalances equivalent to as much as 0.25 pu leakage current.

These simulations concentrate data at lower values, since such values will likely be more important when detecting early stages of insulation breakdown. All combinations of deterioration path and level were simulated at each of three different motor load levels, resulting in 822 distinct system conditions represented in the modeling of each motor. For each of these system conditions, up to four separate samples were taken, yielding data bases containing more than 3,300 observations for a single motor. The use of several samples for each condition creates a more realistic data base by introducing random variations that are normally present in motor terminal measurements. Typically, one or two of the observations for each condition were used in training an ALN, and one was reserved for evaluating the ALN. These were chosen arbitrarily as the first or first and second from those available, depending on the weight desired for the specific condition.

PNETTR modeling of the empirical data just described employed various user controls to optimize the resulting ALN's. These controls included elimination of inappropriate independent variables (such as variables that were phase-dependent, or unstable, or to which a model was too sensitive), limiting the number of ALN layers (to avoid overly complex or sensitive models), and varying model accuracy criteria.

The predicted squared error, a value used by PNETTR to quantify model accuracy, was used as a relative indication of model quality among different versions of the same ALN, while the root mean square (rms) error for an evaluation data set indicated accuracy in determining deterioration level. The latter is the rms of residuals between the actual and model-calculated deterioration levels for a set of observations not used in training the ALN. ALN evaluations were carried out using data for all deterioration levels, and with data representing only 0.00- to 0.10-pu levels.

In addition to collecting more data at lower deterioration levels as previously described, observations for deterioration levels of 0.00 to 0.10 pu were individually given twice the weight of those for 0.15-, 0.20-, and 0.25-pu levels (by including twice as many observations) to enhance model accuracy at the lower levels.

ALN development ultimately focused on 10-, 50-, 100-, and 150-hp motors. Motors used for data generation were Reliance Electric open construction design B machines operating at 460 V, three-phase, with full load currents of 12.2, 62, 120, and 173 A, respectively. PNETTR modeling selected the most appropriate electrical parameters from their respective data bases, and created two optimized ALN's for each motor, one calculating simulated leakage current and the other calculating power dissipated in the leakage path. Table 3 shows the accuracies (rms errors) for each pair of ALN's, using evaluation data as indicated.

For further modeling, data from the 50-, 100-, and 150-hp motors were combined and a single pair of ALN's was created, applicable to this range of motor sizes. Table 4 shows the accuracies (rms errors) for the ALN pair created using the combined data just described. Evaluation results are for 0.00 to 0.10 pu leakage, and are listed for each motor individually.

[5]Per unit (pu) is a method of quantifying electrical values wherein all values are expressed in relation to preselected base quantities defined as 1.0 pu. In this specific case, bases are motor full load values of line to neutral voltage, line current, and complex power. As an example, a line current of 60 A on a motor with a full load current of 120 A would be a line current of 0.50 pu. Note that per unit is a dimensionless quantity.

Comparing tables 3 and 4 shows the "all-motor" ALN pair to be nearly as accurate as the motor-specific ALN's. Given the comparable performance, an ALN pair suitable for a range of motor sizes would likely be more versatile for actual motor monitoring. Therefore, further description and analysis will focus on the ALN's generated from combined 50-, 100-, and 150-hp data.

Table 3.—Root mean squares of residuals between actual and ALN-calculated deterioration values, for motor-specific ALN's

Motor, hp	Current, pu	Power, pu
EVALUATION DATA FOR ALL LEAKAGE LEVELS		
10	0.027	0.013
50	.026	.013
100	.025	.014
150	.025	.013
EVALUATION DATA FOR 0.000- TO 0.10-pu LEVELS		
10	0.019	0.012
50	.019	.012
100	.019	.014
150	.019	.013

Table 4.—Root mean squares of residuals between actual and ALN-calculated deterioration values, for ALN pair created using combined 50-, 100-, and 150-hp data

Data	Current, pu	Power, pu
50-hp	0.018	0.013
100-hp	.020	.015
150-hp	.019	.014

The exact form of these ALN's is shown below.

Deterioration current ALN:

$$X_7 = A_1 + A_2X_1 + A_3X_5 + A_4X_1X_5 + A_5X_1^2 + A_6X_5^2 + A_7X_1^3 + A_8X_5^3,$$

and

$$Y_1 = A_9 + A_{10}X_7 + A_{11}X_2 + A_{12}X_3 + A_{13}X_2X_3 + A_{14}X_7^2 + A_{15}X_2^2 + A_{16}X_3^2 + A_{17}X_7^3 + A_{18}X_2^3.$$

Deterioration power ALN:

$$X_8 = A_{19} + A_{20}X_1 + A_{21}X_2 + A_{22}X_4 + A_{23}X_1X_2 + A_{24}X_1X_4 + A_{25}X_1^2 + A_{26}X_2^2 + A_{27}X_1^3 + A_{28}X_2^3,$$

and

$$Y_2 = A_{29} + A_{30}X_8 + A_{31}X_6 + A_{32}X_8X_6.$$

Where X_1 = negative sequence current polar magnitude,

X_2 = negative sequence current polar angle,

X_3 = negative sequence current x-coordinate,

X_4 = negative sequence current y-coordinate,

X_5 = zero sequence current polar magnitude,

X_6 = three-phase average of real power,

X_7 = first-layer output for deterioration current ALN,

X_8 = first-layer output for deterioration power ALN,

Y_1 = deterioration current level,

Y_2 = deterioration power level,

and A_1-A_{32} = coefficients.

The appendix contains full details for the use of the above ALN, including coefficients and the scaling expressions required for variables.

Figures 6 and 7 illustrate the relationships between input parameters selected by PNETTR and calculated outputs, using the above ALN's for two specific deterioration conditions on the 150-hp motor running unloaded. These two cases are representative of similar plots for other conditions. Note the importance of negative sequence current components as variables in both ALN's. This is logical since negative sequence current is a direct measurement of line current imbalance and, therefore, indicates electrical imbalance present on a motor.

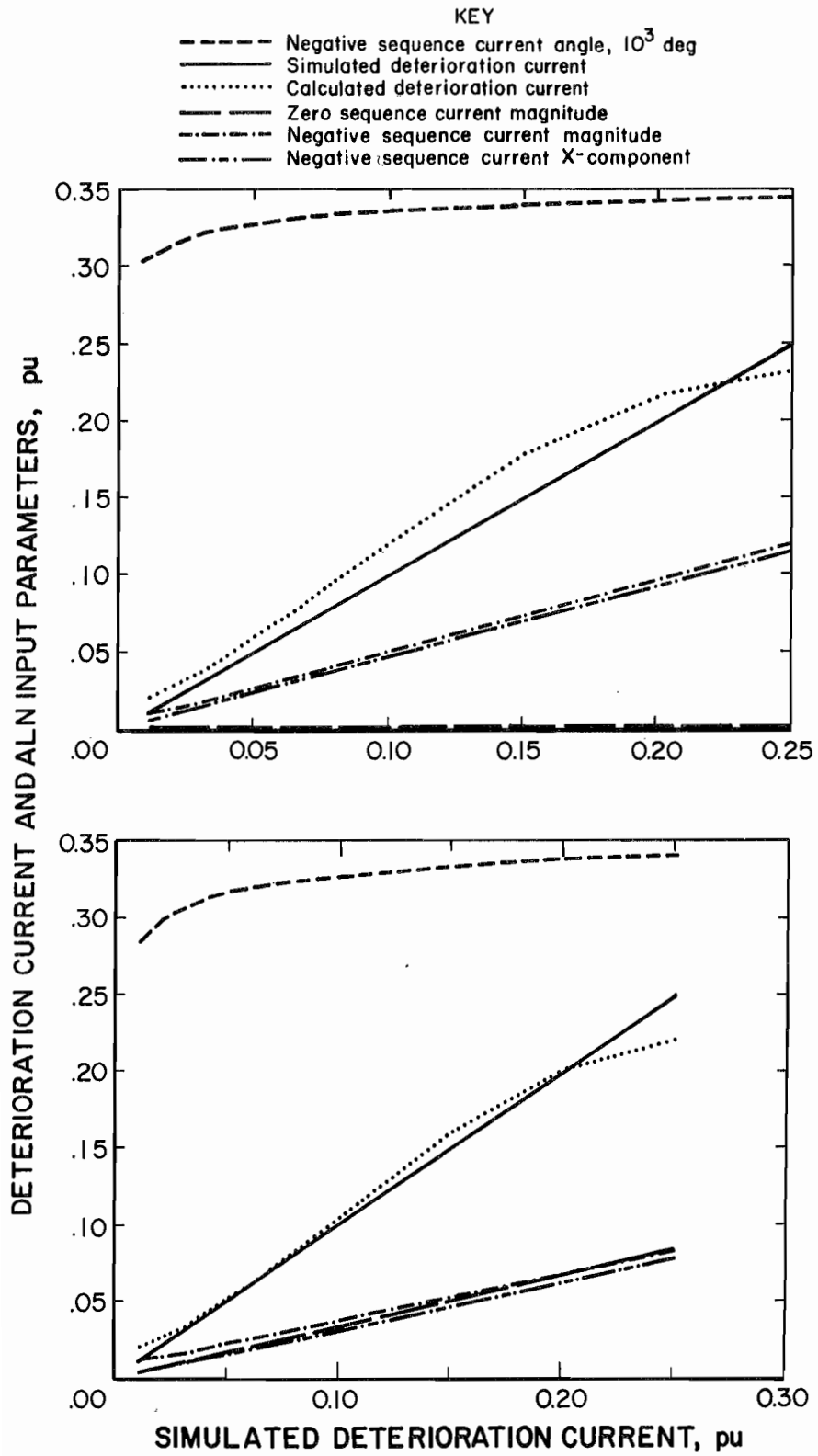

Figure 6.—Relationship of ALN input parameters to calculated deterioration current, for simulated A-b (top) and A-G (bottom) leakage on 150-hp motor running unloaded.

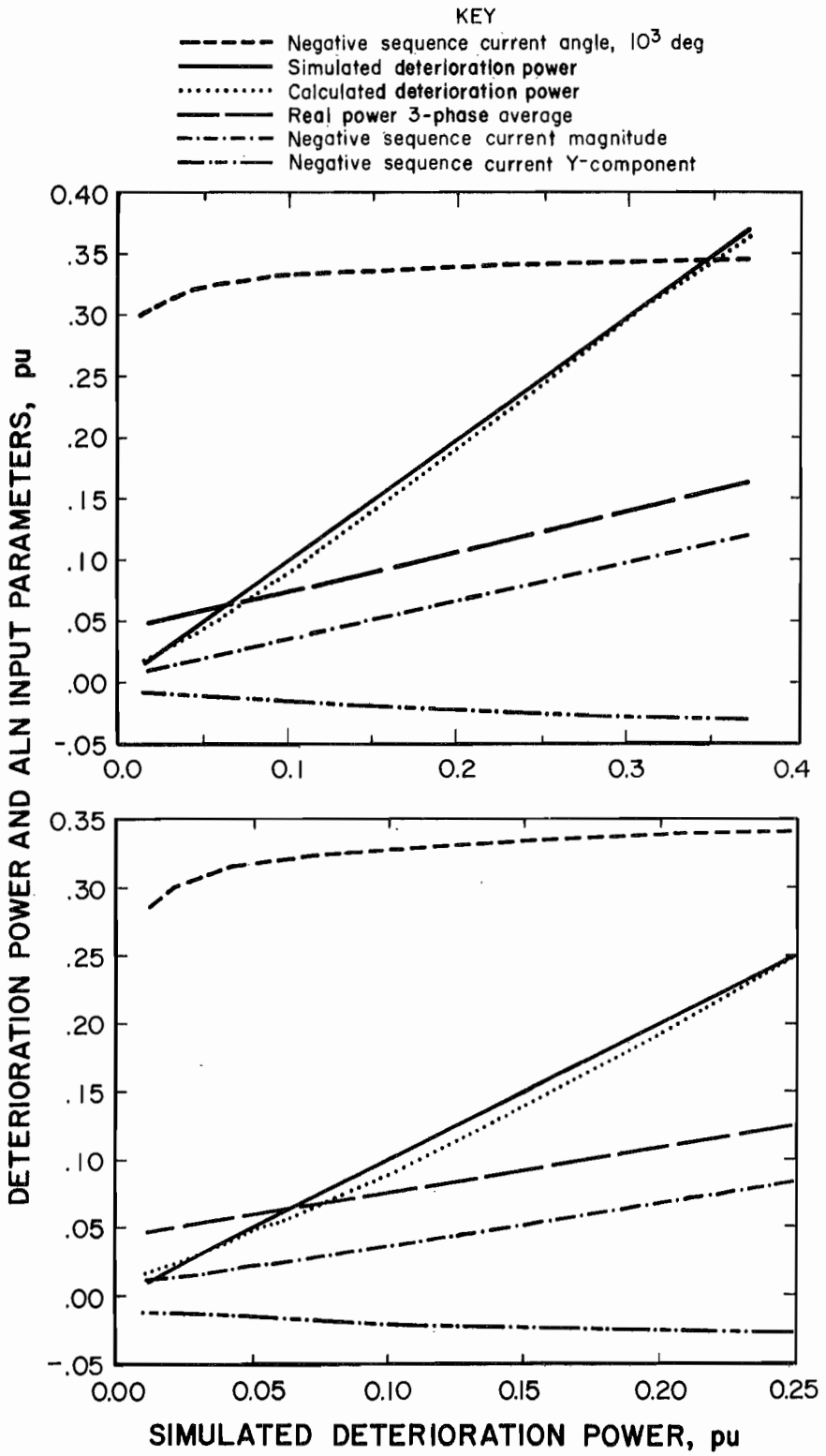

Figure 7.—Relationship of ALN input parameters to calculated deterioration power, for simulated A-b (top) and A-G (bottom) leakage on 150-hp motor running unloaded.

The rms values in table 4 indicate overall accuracy for the ALN's, but figures 8 and 9 illustrate in more detail the influence of deterioration type and level on ALN performance. These figures plot the deviation of ALN-calculated leakage levels from known actual leakage levels (laboratory simulations) for six different leakage paths on the 150-hp motor running unloaded. The cases chosen are representative of overall ALN performance.

Figures 10 and 11 are similar plots, showing the effect of motor load level on ALN performance. The condition represented is A-G leakage on the 150-hp motor, and again, is generally representative of other conditions.

Winding temperature has a significant effect on conventional insulation resistance testing techniques used to assess motor electrical condition. The ALN's developed under this work, however, are not adversely affected by motor temperature changes, since results are based on parameters that represent motor electrical imbalance, not actual winding insulation impedance values. Figure 12 illustrates this temperature independence by showing ALN outputs calculated using data taken from a laboratory 100-hp motor, at full load, from 35° C to 85° C winding temperature, while undergoing simulated A-B winding leakage.

SUMMARY

The important findings of the foregoing discussion follow:

- PNETTR modeling of motor systems can create functions, ALN's, that accurately detect and quantify simulated motor winding insulation leakage from measurable electrical parameters.
- These ALN's can be used to detect and quantify simulated insulation leakage without regard for leakage path location and severity, motor load level, or winding temperature.
- A single ALN can accurately evaluate simulated leakage on motors of several different sizes, specifically in this research, 50-, 100-, and 150-hp motors.

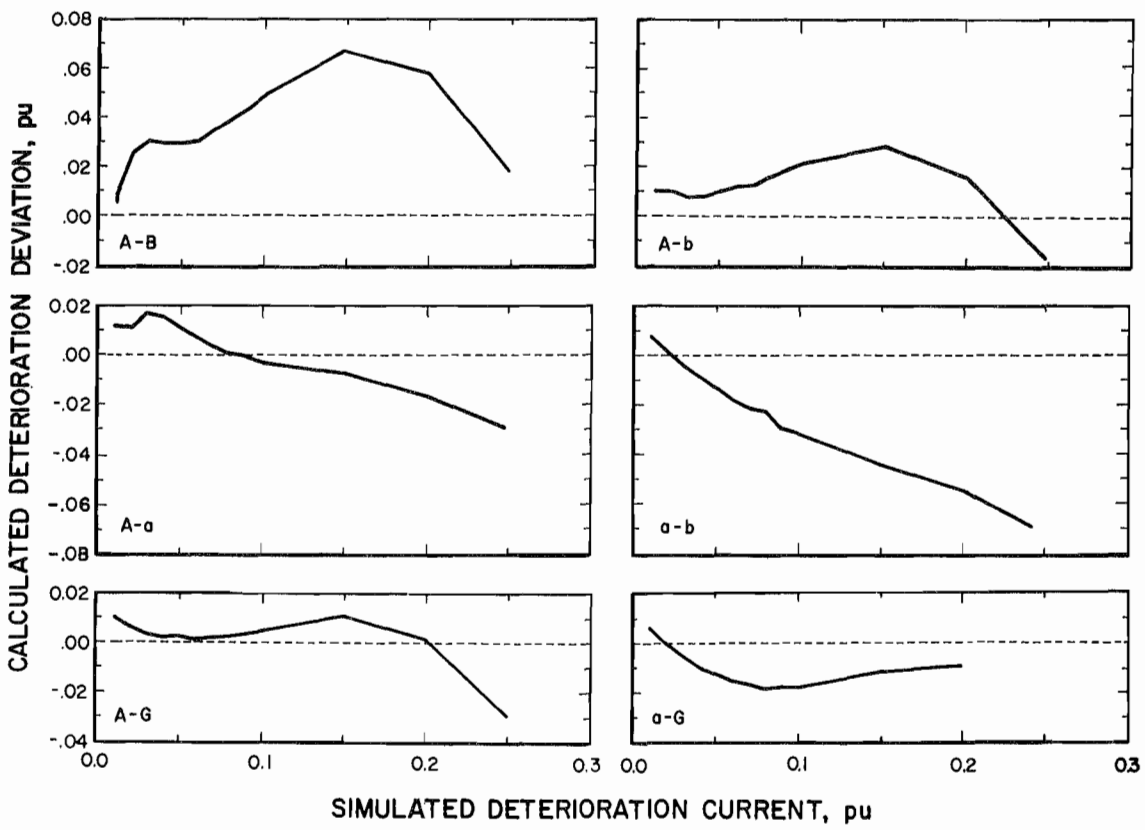

Figure 8.—Deviation of ALN-calculated deterioration current from actual simulated deterioration current, for leakage on 150-hp motor running unloaded.

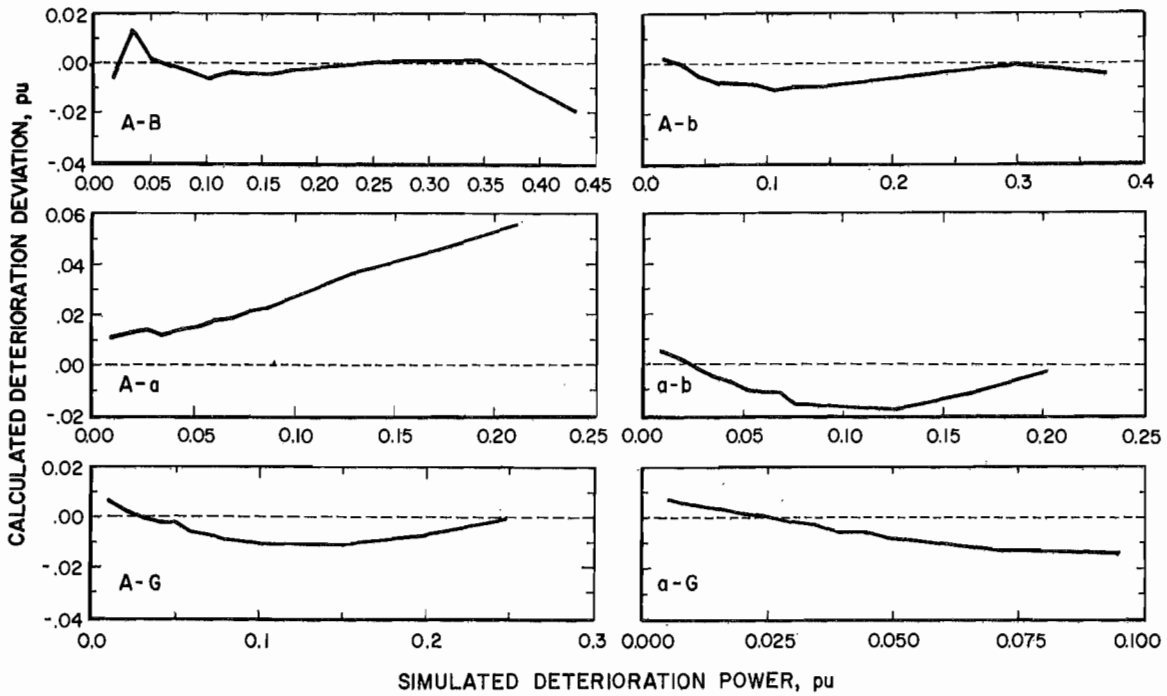

Figure 9.—Deviation of ALN-calculated deterioration power from actual simulated deterioration power, for leakage on 150-hp motor running unloaded.

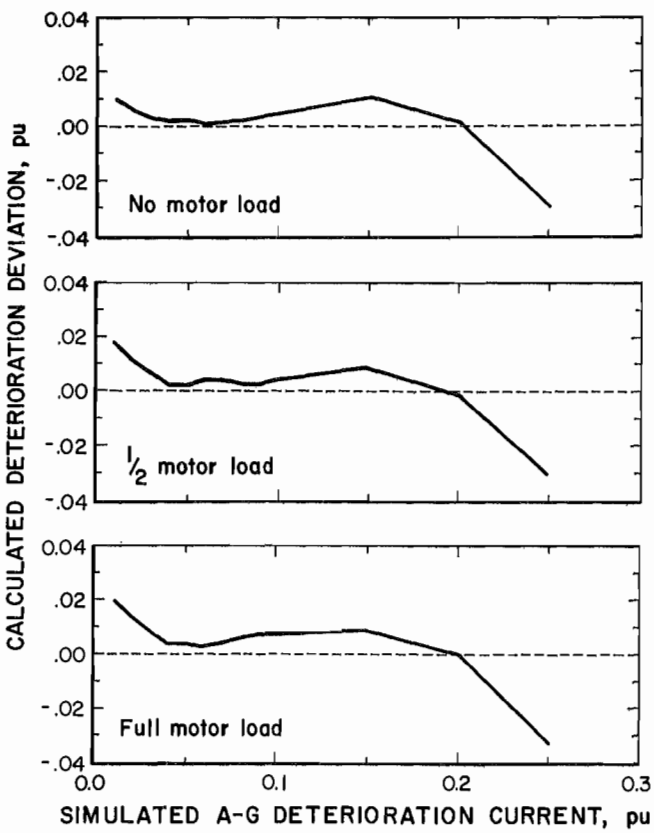

Figure 10.—Deviation of ALN-calculated deterioration current from actual simulated deterioration current, for A-G leakage on 150-hp motor running with various loads.

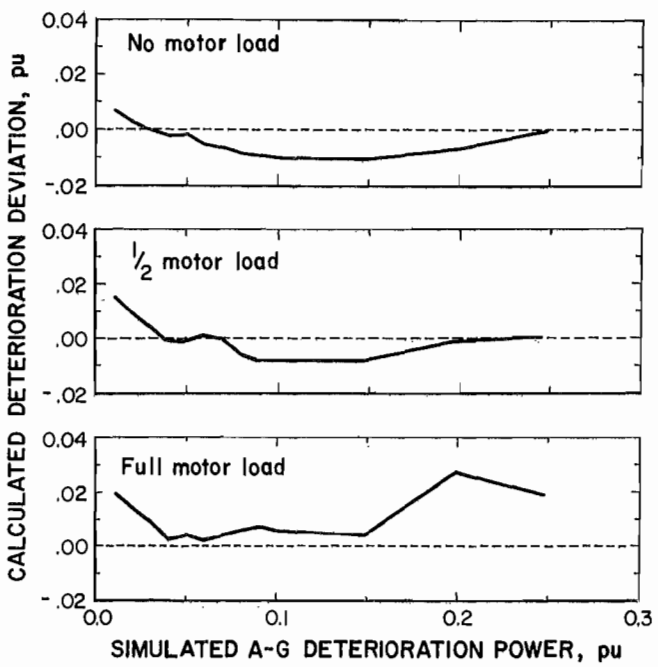

Figure 11.—Deviation of ALN-calculated deterioration power from actual simulated deterioration power, for A-G leakage on 150-hp motor running with various loads.

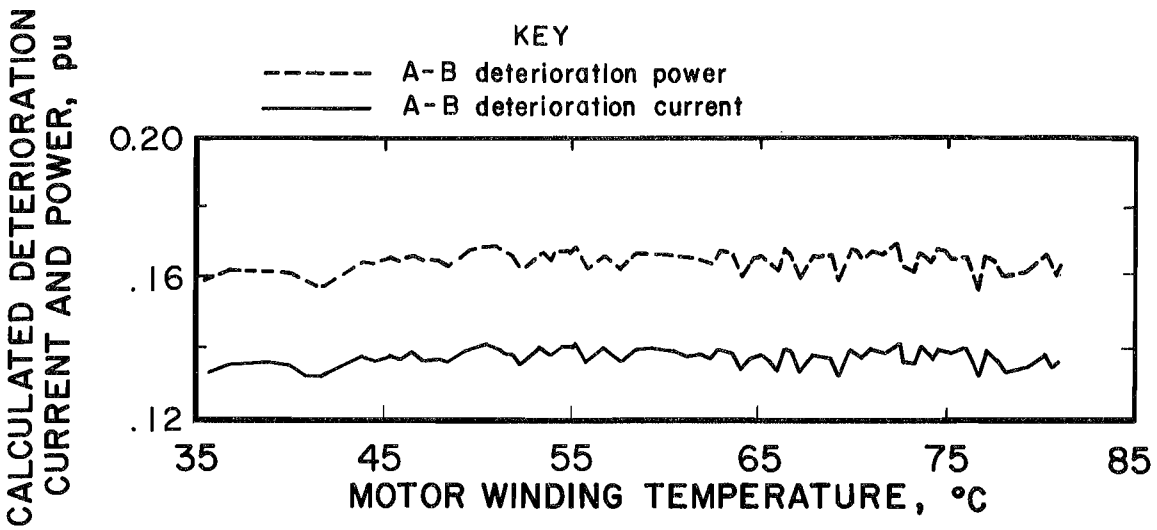

Figure 12.—Effect of motor temperature change on ALN-calculated deterioration, for simulated A-B leakage on 100-hp motor running at full load.

ACCELERATED LIFE MOTOR TESTING

GENERAL

Failure detection techniques have been developed using simulated deterioration conditions. This is based on the assumption that in actual motor failure, insulation degradation is gradual and of sufficient magnitude to allow early detection.

To validate this assumption, ongoing work includes accelerated life testing of motors. These tests attempt to induce gradual insulation failure in laboratory motors to confirm the presence of detectable insulation breakdown prior to motor failure. In these tests, typical mine equipment motors are operated at above-normal temperatures to accelerate winding insulation degradation. Motor electrical parameters are recorded at regular intervals during this deterioration process, and deterioration current and power levels are calculated using ALN's. The results are analyzed to identify unique signatures present prior to complete motor failure. Carefully controlled acceleration of motor aging will permit the completion of this work in a practical time frame, while allowing extrapolation of results to motor life under normal operating conditions.

EXPERIMENTAL DESIGN

IEEE Standard 117-1974 (*6*) specifies procedures for accelerated aging of motor insulation. This document prescribes electrical, mechanical, and thermal stress for the rapid degradation of insulation in both complete motors and motorettes. The standard, however, is primarily concerned with the determination of time to end of life for motor insulation, while the objective of this research is to induce gradual failure. Therefore, in this testing, only thermal stress is imposed upon motor insulation systems. This does not imply that thermal conditions are more significant than others, but was done to allow better control over the accelerated aging rate, as well as to avoid the catastrophic failures that can occur as test specimens are subjected to cycles of thermal, mechanical, and electrical abuse. Since the purpose of these tests and this approach to motor insulation aging are unique, little information for experimental design and procedures is available in existing standards. As a result, many aspects of the necessary laboratory work require refinement as testing progresses.

Test motors are operated at full load while exposed to elevated ambient temperatures, with expected motor insulation life reduced by half for each 10° C rise above maximum rated operating temperature. Using a normal life expectancy of 40,000 h and class F insulation rated at 155° C maximum, estimated motor insulation lives at various temperatures are listed below (*7*).

Life, h	*Temperature, °C*
20,000	165
10,000	175
5,000	185
2,500	195
1,250	205
625	215
312	225

Motors used are Reliance Electric 20-hp, design B, squirrel cage induction machines, with Mine Safety and Health Administration (MSHA)-approved explosion-proof enclosures. A metal chamber equipped with four 750-W heating elements is used to elevate motor ambient temperature, thereby raising internal insulation temperatures. Figure 13 shows the motor-alternator set with the heat chamber open. Thermocouples and a programmable data logger are used to monitor temperatures in and around test motors and to provide a control loop for the heating elements. Thermocouple placements include chamber ambient, windings (near end of stator slots), and the outer race of each bearing. Instrumentation provides for monitoring of line-to-line voltages and line currents at motor terminals. These signals are collected, processed, and stored using a desk-top-computer data-acquisition system. This system, based on a distributed processing network, uses remote monitoring stations to sample, digitize, and process motor terminal values, and then transmit voltage and current phasors back to a central computer for storage. Subsequent analysis uses the most appropriate available ALN. Figure 14 is an illustration of the complete layout for this testing. Motor insulation condition is also evaluated using insulation resistance (IR) measurements at regular intervals during testing, and the results of this conventional technique are compared with those of ALN processing.

Figure 13.—Motor-alternator set for accelerated aging of motor insulation, shown with heat chamber open. (Photo credit: R. Wayne Denlinger, engineering technician, Pittsburgh Research Center.)

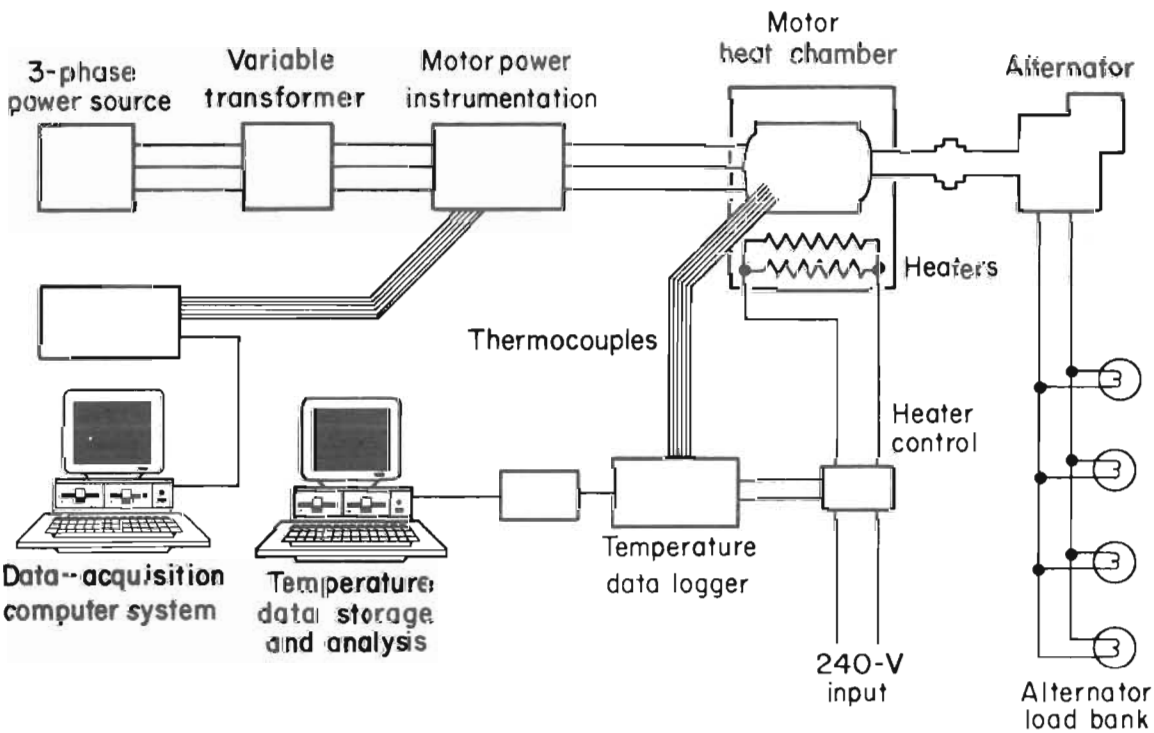

Figure 14.—Layout of laboratory equipment for motor insulation accelerated life testing.

PRELIMINARY RESULTS

The first test motor run to failure in this work did not yield data from which signs of impending motor failure could be identified. It did, however, provide valuable information for refinement of experimental equipment and procedures. Several changes resulting from this test were the replacement of magnetic tape recording with computer-based digital data acquisition, improvements in organization and storage of motor and temperature data, addition of a high common mode voltage (surge) rejection circuit to the temperature data logger, revised bearing lubrication practices, and improvement in motor to alternator coupling.

Of particular interest was determination of the temperature gradient from heat chamber ambient to motor housing and bearings and, finally, to the motor windings. This information guided selection of cable insulation ratings, temperature ratings of other materials used in the heat chamber, and maximum rating of the grease used in the motor bearings. The temperature gradient observed is shown in table 5.

Table 5.—Temperature gradient observed

Monitoring point	*Approximate temperature, °C*
Motor winding (in slot, near end)	215
Motor case (inside surface)	175-180
Bearing, load end (outer race)	175
Bearing, fan end (outer race)	170
Heat chamber ambient (center near top)	145
Alternator bearing (end cap surface)	60

A second test motor was run at a winding temperature of 215° C; it failed after approximately 900 h of operation, reasonably approximating the life predicted by the aforementioned 10° C rule. The ALN analysis of associated motor terminal data, however, did not provide early warning of the failure. Conventional IR measurements, conducted 15 h prior to failure, also gave no indication of the impending insulation breakdown.

Measurements made after failure indicated low resistance paths between all phase windings, and between all windings and ground. The motor was then sent to Reliance Electric for analysis to determine the mode and cause of failure. The following is a summary of their findings.

- Time to failure correlated closely with Reliance Electric projections based on their motor insulation material tests.
- Many materials present in the motor were discolored and/or embrittled by the high test temperatures.
- Failure occurred in the first coil downline from a motor terminal, approximately 1 inch out from the edge of the stator core.
- Failure began as a turn-to-turn short within the coil, progressed to phase-to-phase with an adjacent coil, and finally failed to ground (this progression was not a result of high current during motor starting, since no attempt was made to restart the motor after the initial failure).
- Immediate failure area showed signs of significant burning.
- Insulation on winding wire had longitudinal and circumferential cracking.
- Failure was caused by embrittlement and cracking of winding wire insulation, as a result of high operating temperature and normal operating vibration.

In a discussion of these analysis results with a Reliance Electric engineer, possible changes to accelerated life testing procedures were suggested.

The failure of IR measurements to detect the breakdown (cracking) of insulation may be due to extremely dry conditions inside the motor as a result of the high operating temperatures. Higher humidity inside the motor during IR tests would likely reveal a progressive drop in insulation integrity prior to complete failure. Although it would be difficult to control humidity and condensation conditions inside a motor during operation, increasing the moisture present may also aid in detection of time-dependent deterioration using ALN's; this possibility will be investigated further.

The location of the failure, on the first coil downline from a motor terminal, suggests that a fast-rise-time voltage transient may have triggered the failure. Monitoring of the laboratory three-phase power system confirmed the presence of voltage transients as high as 670 V with durations up to 100 μs. In order to avoid catastrophic failure of weakened insulation systems in the future, a surge suppression device will be installed to protect the test motors.

It is also possible that a winding temperature of 215° C is too severe to allow accelerated yet gradual deterioration of motor insulation, or that the sudden and complete failure of this motor was simply an anomaly.

At this writing, a third and fourth motor are under test, both at winding temperatures of 205° C.

CONCLUSIONS

The first stage in research to develop a practical motor condition monitoring system has been completed. ALN's developed under this work can detect the presence and severity of simulated insulation leakage independent of leakage position and level, motor load, and motor temperature. A single pair of ALN's can yield accurate results for motors of varying size, specifically 50-, 100-, and 150-hp motors.

The feasibility of ALN-based failure detection relies upon verification of the relationship between gradual insulation breakdown and ultimate complete motor failure. The second stage of this research has been initiated to establish and quantify this relationship through accelerated life testing of motors. Laboratory experimentation induces insulation failure by accelerated aging, while monitoring terminal information for early signs of impending failure. This work has not yet yielded conclusive results.

REFERENCES

1. Morley, L. A., and J. L. Kohler. Final Report—Evaluation of Coal-Mine Electrical-System Safety (grant G0155003, PA State Univ.). BuMines OFR 160-81, 1981, 258 pp.; NTIS PB 82-139338.

2. Kohler, J. L. A Decision-Theoretic Method for the Classification of Incipient-Failure Patterns Which Are Characteristic of Deteriorating Mine Power-System Components. Ph.D. Thesis, PA State Univ., University Park, PA, 1983, 141 pp.

3. Kohler, J. L., and F. C. Trutt. Prediction of Incipient Electrical-Component Failures (contract J0338028, PA State Univ.). BuMines OFR 35-88, 1987, 370 pp.; NTIS PB 88-213590.

4. General Research Corp. (McLean, VA). PNETTR-4X User's Guide and Technical Reference. Aug. 1986, 74 pp.

5. Morley, L. A. Mine Power Systems. BuMines IC 9258, 1990, 437 pp.

6. Institute of Electrical and Electronic Engineers. IEEE Standard Test Procedure for Evaluation of Systems of Insulating Materials for Random-Wound A C Electric Machinery. IEEE Std. 117-1974, 1974, 24 pp.

7. General Electric Technical Services Co. (Plainville, CT). Motor Temperature Ratings and Construction Tech. Pam. E-19, 1974, 5 pp.

APPENDIX.—ALN IMPLEMENTATION DETAILS

The equations below outline the form of the ALN's developed using combined data from 50-, 100-, and 150-hp motors.

Deterioration current ALN:

$$X_7 = A_1 + A_2X_1 + A_3X_5 + A_4X_1X_5 + A_5X_1^2 + A_6X_5^2 + A_7X_1^3 + A_8X_5^3,$$

and

$$Y_1 = A_9 + A_{10}X_7 + A_{11}X_2 + A_{12}X_3 + A_{13}X_2X_3 + A_{14}X_7^2 + A_{15}X_2^2 + A_{16}X_3^2 + A_{17}X_7^3 + A_{18}X_2^3.$$

Deterioration power ALN:

$$X_8 = A_{19} + A_{20}X_1 + A_{21}X_2 + A_{22}X_4 + A_{23}X_1X_2 + A_{24}X_1X_4 + A_{25}X_1^2 + A_{26}X_2^2 + A_{27}X_1^3 + A_{28}X_2^3,$$

and

$$Y_2 = A_{29} + A_{30}X_8 + A_{31}X_6 + A_{32}X_8X_6.$$

Where X_1 = negative sequence current polar magnitude,

X_2 = negative sequence current polar angle,

X_3 = negative sequence current x-coordinate,

X_4 = negative sequence current y-coordinate,

X_5 = zero sequence current polar magnitude,

X_6 = three-phase average of real power,

X_7 = first-layer output for deterioration current ALN,

X_8 = first-layer output for deterioration power ALN,

Y_1 = deterioration current level,

Y_2 = deterioration power level,

and A_1-A_{32} = coefficients.

In order to use the above equations, all input variables, expressed in per unit or degrees, must be "scaled" according to the following procedure (using X_0 as an example input variable).

$$X_0 \text{ scaled} = \frac{X_0 \text{ actual} - X_0 \text{ mean}}{X_0 \text{ standard deviation}}.$$

First-layer output variables X_7 and X_8 do not need to be scaled for use in the second layers.

The above scaling procedure is then reversed to derive per unit deterioration values from raw (scaled) Y_1 and Y_2 ALN outputs. This is shown here (using Y_0 as an example output variable).

$$Y_0 \text{ actual} = [(Y_0 \text{ scaled}) \times (Y_0 \text{ standard deviation})] + Y_0 \text{ mean}.$$

The means and standard deviations are calculated from ALN training data, and are listed below for independent variables X_1 through X_6, Y_1, and Y_2.

Variable	*Mean*	*Standard deviation*
X_1	0.028191	0.022119
X_2	225.54	89.43
X_3	-0.00035328	0.023794
X_4	-0.012098	0.023904
X_5	0.0090997	0.013913
X_6	0.48197	0.32284
Y_1	0.071010	0.057294
Y_2	0.074930	0.070016

ALN coefficients are listed below.

A_1 = -0.18894
A_2 = 0.73500
A_3 = 0.06757
A_4 = -0.19559
A_5 = 0.13119
A_6 = 0.18665
A_7 = -0.03381
A_8 = -0.01405
A_9 = -0.14007

A_{10} = 1.03196
A_{11} = -0.28485
A_{12} = -0.05990
A_{13} = -0.01962
A_{14} = 0.01665
A_{15} = 0.26385
A_{16} = 0.00974
A_{17} = -0.02165
A_{18} = 0.11437
A_{19} = -0.16743
A_{20} = 0.86996
A_{21} = -0.32337
A_{22} = 0.15622
A_{23} = 0.00446
A_{24} = -0.03063
A_{25} = 0.09912
A_{26} = 0.22836
A_{27} = -0.01579
A_{28} = 0.12995
A_{29} = -0.00116
A_{30} = 0.99587
A_{31} = 0.02508
A_{32} = 0.02515

INT.BU.OF MINES,PGH.,PA 29701

*U.S.G.P.O.: 1993--709-008/60104